metals

Article

Microstructures and Mechanical Properties of Austempering SUS440 Steel Thin Plates

Cheng-Yi Chen, Fei-Yi Hung *, Truan-Sheng Lui and Li-Hui Chen

Department of Materials Science and Engineering, National Cheng Kung University, Tainan 701, Taiwan; n5897115@mail.ncku.edu.tw (C.-Y.C.); luits@mail.ncku.edu.tw (T.-S.L.); chenlh@mail.ncku.edu.tw (L.-H.C.)
* Correspondence: fyhung@mail.ncku.edu.tw; Tel.: +886-6-2757575 (ext. 62950); Fax: +886-6-2346290

Academic Editor: Hugo F. Lopez
Received: 30 November 2015; Accepted: 30 January 2016; Published: 15 February 2016

Abstract: SUS440 is a high-carbon stainless steel, and its martensite matrix has high heat resistance, high corrosion resistance, and high pressure resistance. It has been widely used in mechanical parts and critical materials. However, the SUS440 martempered matrix has reliability problems in thin plate applications and thus research uses different austempering heat treatments (tempering temperature: 200 °C–400 °C) to obtain a matrix containing bainite, retained austenite, martensite, and the M7C3 phase to investigate the relationships between the resulting microstructure and tensile mechanical properties. Experimental data showed that the austempering conditions of the specimen affected the volume fraction of phases and distribution of carbides. After austenitizing heat treatment (1080 °C for 30 min), the austempering of the SUS440 thin plates was carried out at a salt-bath temperature 300 °C for 120 min and water quenching was then used to obtain the bainite matrix with fine carbides, with the resulting material having a higher tensile fracture strength and average hardness (HRA 76) makes it suitable for use as a high-strength thin plate for industrial applications.

Keywords: stainless steel; austempering; bainite; mechanical properties

1. Introduction

SUS440 is a high-chrome and carbon martensite stainless steel with high strength and corrosion resistance properties and thus been widely used in machine parts, screws, and knives [1,2]. In general, martensite stainless steel almost always undergoes austenitizing heat treatment, followed by quenching and tempering. However, if this process is carried out improperly, then this will adversely affect the mechanical properties of the resulting materials [3,4]. This is because the quenching rate and temper-brittleness, and especially quench-tempering, can lead to reliability problems with regard to thin plates [5,6]. In the current study, SUS440 plate is made into a double-loop type thin plate specimen by a punch-shear process, in order to highlight the stress concentration and study the effects on brittleness. Austempering heat treatment can produce excellent mechanical properties in iron-based materials [7,8], although the characteristics of austempered SUS440 have still not been studied. Notably, the salt that was used in the current study can also meet the demand for a more environmentally-friendly process [9]. Therefore, this research controlled the heat treatment conditions (Ms temperature is about −40 °C [10]) to obtain SUS440 with a bainite matrix, retained austenite, and stable MC carbides, and then investigated the tensile strength and hardness of this material in order to obtain data for use in SUS440 thin plate applications [11].

2. Experimental Procedure

The chemical composition of SUS440 is given in Table 1, the carbon content is 0.75% by mass, the chrome content is 18% by mass, and it contains other alloying elements, such as Si, Mn, and V.

This research uses a double loop-type thin plate (t = 0.78 mm) specimen to examine the effects of the punch-shear process on brittleness. Figure 1 shows the dimensions of the specimen. Figure 2 shows a diagram of the austempering process. The heat treatment condition of the specimen was 1080 °C (vacuum) held for 30 min for austenitic treatment (the austenite conditions of all specimens are the same), and then the specimen was immediately moved into a salt-bath furnace for austempering. There were two different conditions for the salt-bath phase and thus two sets of specimens were prepared. The first set underwent the same salt-bath time (120 min) and different constant temperatures (200, 300, and 400 °C), and were then quenched in the water. The second set underwent the same salt-bath temperature (300 °C) and different time intervals (30, 60, 90, and 120 min), and were then quenched in the water. Each austempering condition was called x °C-y min, based on the salt-bath condition, such as 200 °C-120 min [7,8].

Table 1. The chemical composition of the SUS440 (mass %).

Element	C	Mn	Si	P	S	V	Cr	Mo	Fe
Content	0.75	1.00	1.00	0.04	0.04	0.15	18.20	0.30	Bal.

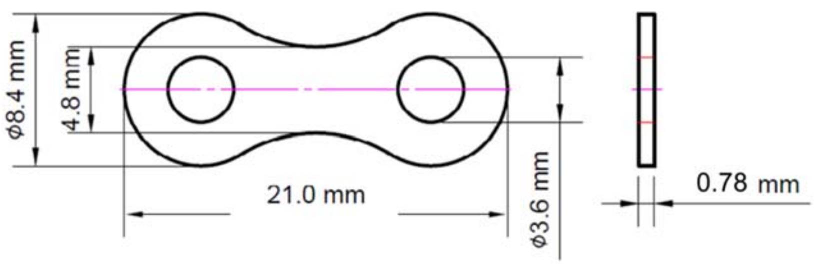

Figure 1. Configuration of a double-loop thin plate specimen.

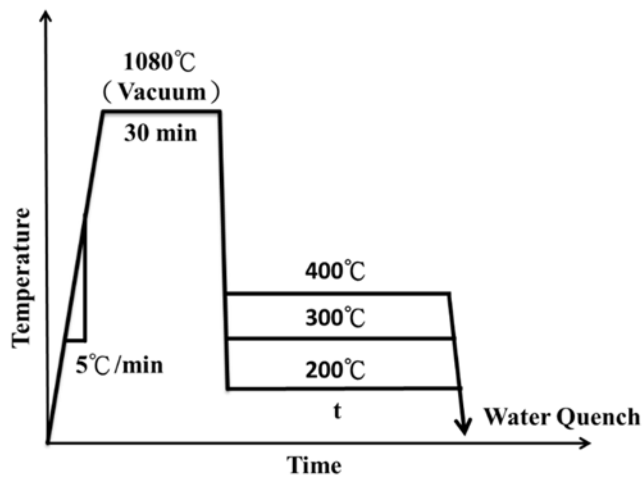

Figure 2. The tempering process with different salt-bath temperatures.

The characteristics of each austempered specimen were determined quantitatively by SEM (Hitachi SU8000, Hitachi, Tokyo, Japan) and an image analyzer (Oxford Instrument, Abingdon, UK). The hardness (HRA) and the tensile properties (tensile rate: 1 mm· min^{-1}) of each specimen were evaluated. The structural phases were identified by XRD (Bruker AXS, Karlsruhe, Germany). The short (30 min) and long (120 min) tempering affected the precipitation of the tempering carbides, and Electron Spectroscopy for Chemical Analysis (ESCA, PHI 5000 V, ULVAC-PHI, Inc., Kanagawa, Japan) was used to assess this. In addition, SEM and OM were used to observe the fracture surface and subsurface of the specimen to clarify the tensile failure characteristics of thin plate specimens [11].

3. Results and Discussion

Figure 3 shows the microstructures of the austempered bainite specimens (1080 °C-30 min) with different salt-bath conditions. The matrix is the feather bainite structure. Notably, the major phases were the retained austenite phases combined with martensite, and the particles were the carbides. In addition, the salt-bath specimen at 300 °C, became coarser was the austempering duration increased (Figure 4). A fully bainite matrix with finer primary carbides can be achieved with a longer austempering time [5,12–14]. However, if the tempering time was insufficient, then no feathery structure was seen in the matrix after etching.

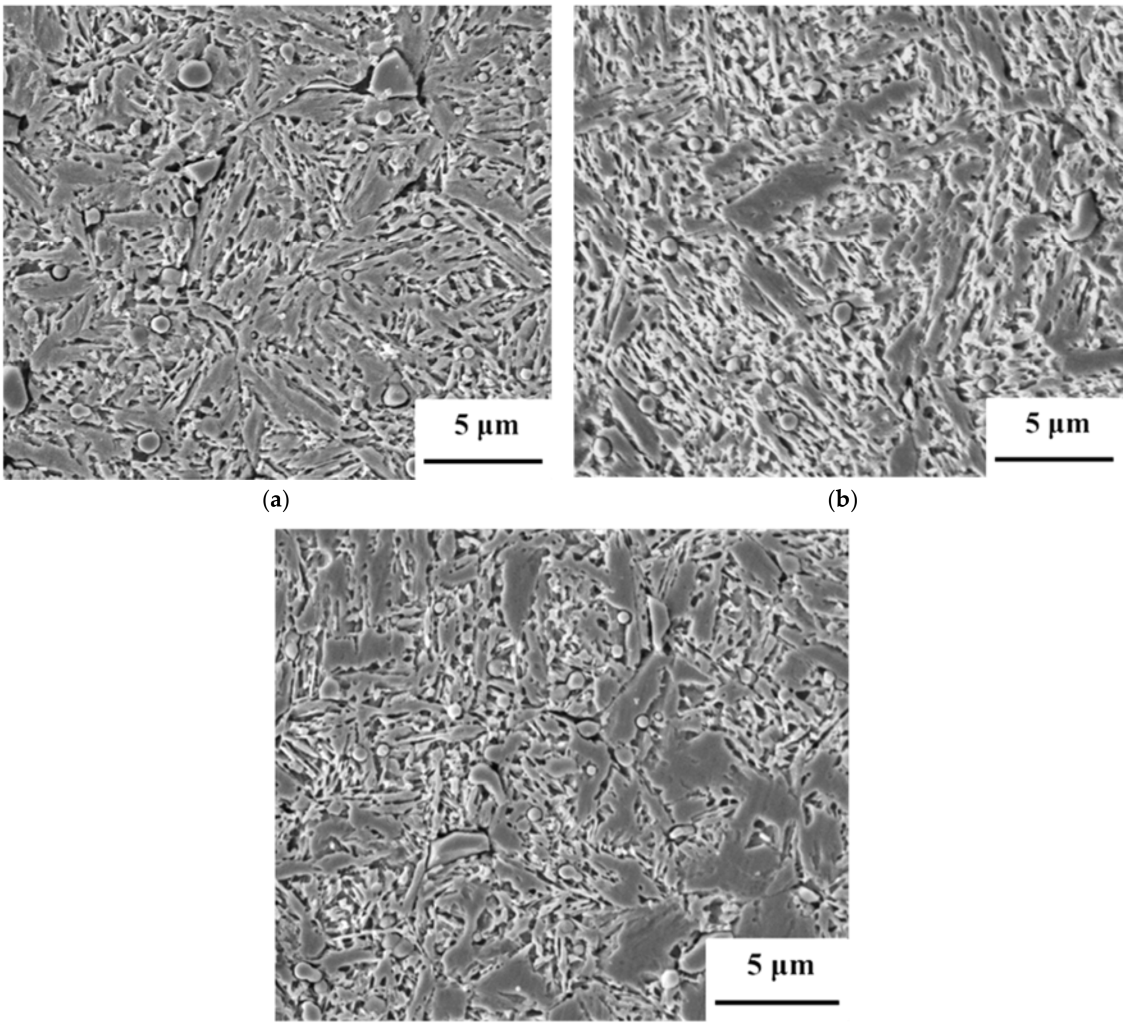

(**a**) (**b**) (**c**)

Figure 3. Microstructural characteristics of the austempered specimens (1080 °C-30 min) with a salt-bath time of 120 min and different salt-bath temperatures: (**a**) 200 °C, (**b**) 300 °C, and (**c**) 400 °C.

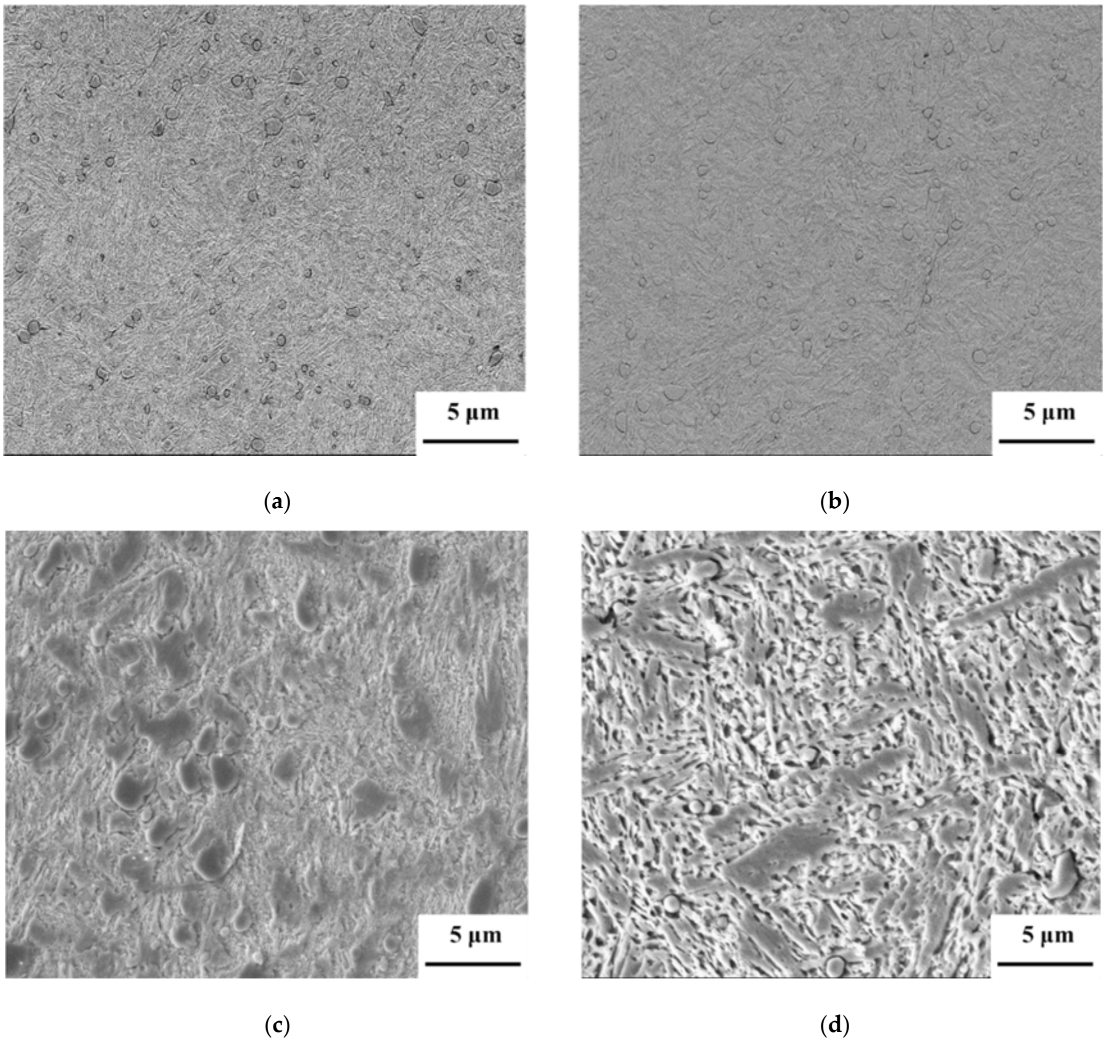

Figure 4. Microstructural characteristics of the austempered specimens (1080 °C-30 min) with a salt-bath temperature of 300 °C and different salt-bath times: (**a**) 30 min, (**b**) 60 min, (**c**) 90 min, and (**d**) 120 min.

The XRD patterns of the specimens produced under different salt-bath conditions after austempering at 1080 °C-30 min, are shown in Figures 5 and 6. All the specimens shown in the figure have a bainite matrix, M7C3 carbide, and retained austenite combining martensite, while the specimen produced at an austempering temperature of 200 °C had more martensite phases [8,15,16]. Figure 5 shows that the retained austenite content of the specimen produced at a salt-bath temperature of 400 °C is the highest, while Figure 6 shows that the austenite content of the specimen decreases as the austempering time increases.

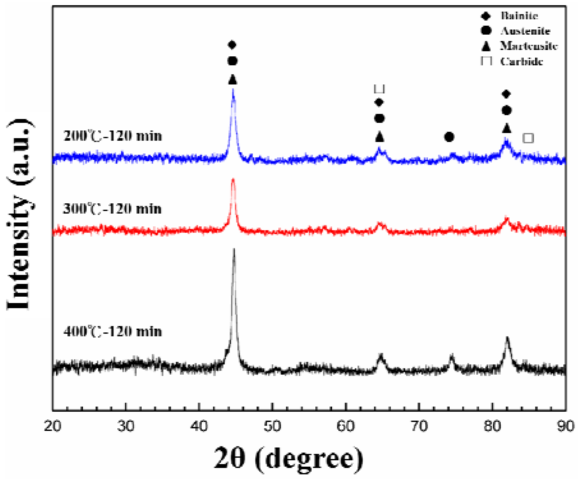

Figure 5. XRD of austempered specimens (1080 °C-30 min) with a salt-bath time of 120 min and different salt-bath temperatures.

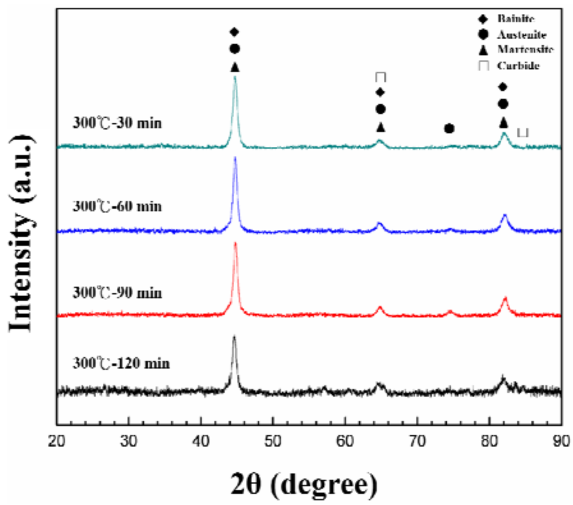

Figure 6. XRD of austempered specimen (1080 °C-30 min) with a salt-bath temperature of 300 °C and different salt-bath time.

Figure 7 is the schematic diagram of the tensile test method in this study we use two pins to insert into the double-loop type thin plate specimen and vertical. Figure 8 shows a comparison of the tensile properties obtained with different salt-bath temperatures. The tensile properties of the 300 °C specimen are significantly better than those of the other specimens. The main reason for this is that the austempering temperature of 200 °C is too low for complete austempering and thus the matrix also contains martensite, which increases the brittleness of the material [5,17,18]. The 400 °C specimen has more retained austenite, which results in lower tensile mechanical properties. In the hardness tests, the 200 °C specimen had greater hardness because of the martensite inside the matrix [2,19], while the other specimens had an HRA of about 76.

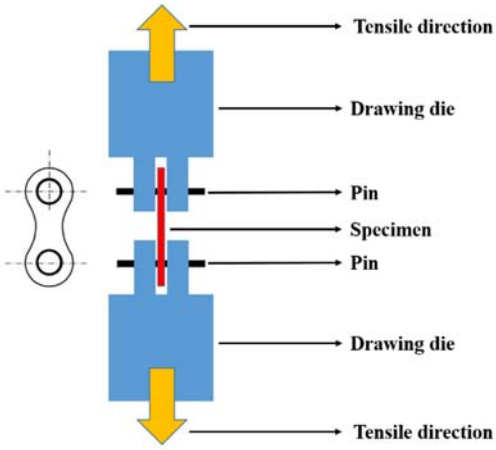

Figure 7. The schematic diagram of the tensile test method.

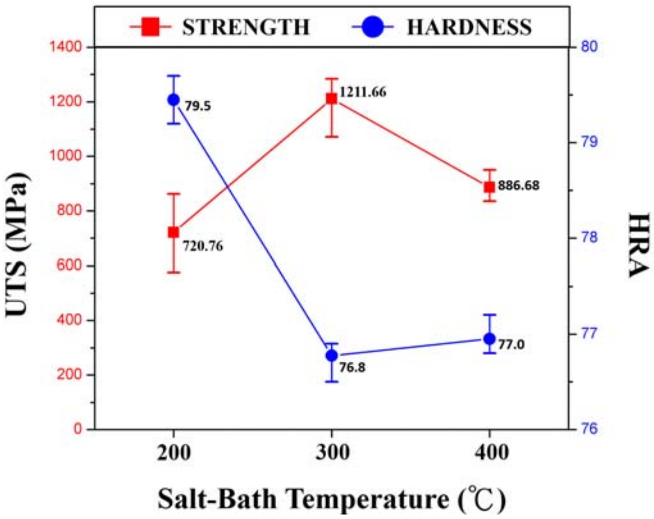

Figure 8. The mechanical properties of the austempered specimens (1080 °C-30 min) with a salt-bath time of 120 min and different salt-bath temperatures.

Figure 9 shows a comparison of the tensile properties for specimens obtained at different salt-bath times (30–120 min, fixed salt-bath temperature at 300 °C) after austenitizing at 1080 °C for 30 min. The average tensile strength of the 90 min specimen was greater than that of the others (>1100 MPa), and the hardness of all four heat treatment conditions was above HRA 76 [17,18]. Therefore, the condition of austenitizing at 1080 °C for 30 min, followed by austempering at salt-bath temperature of 300 °C for 90 min, led to the best tensile properties and hardness (and the composition of the resulting microstructure was 68.8% bainite + 12.6% martensite + 15.5% austenite + 3.1% carbides). The fracture characteristics of the various specimens were then compared using a tensile test.

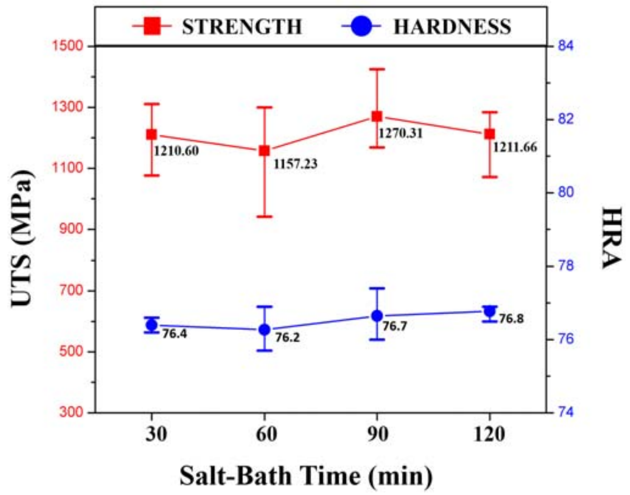

Figure 9. The mechanical properties of the austempered specimens (1080 °C-30 min) with a salt-bath temperature of 300 °C and different salt-bath times.

Figure 10 shows the strain-stress curve of the specimens produced under different salt-bath times (30–120 min, fixed salt-bath temperature at 300 °C) after austenitizing at 1080 °C-30 min. There is no necking characteristics that could be observed, so it is the brittle failure. Figure 11 shows the fracture surfaces of the specimens produced at 300 °C with different austempering durations. It can be seen that there are many peel-off structures, and this confirms the characteristics of ductile-brittle failure (Figure 11a–c). Figure 11d shows the peel-off microstructure, but some splitting behavior also occurred on the fractured surface, and this was due to the brittle fracture mode. Figure 12 shows the subsurface of the 300 °C specimens produced with salt-bath times of 30 min and 120 min. When the matrix was composed of a fine feather structure and martensite and subjected to a short duration (30 min) of austempering, the brittleness became significant and caused the subsurface to become irregular (Figure 12a) [12,20]. Figure 12b shows the flat fracture characteristic that was obtained with a longer austempering time (120 min). Since the austempering duration affected carbide precipitation and the tensile fracture behavior, electron spectroscopy chemical analysis (ESCA) was applied to the austempered SUS440 to measure the carbide contents (Figure 13). With the shorter austempering time (30 min), the main carbides were the M23C6 (M7C3) precipitate phases (Figure 13a). As the austempering time increased (Figure 13b), the content of M23C6 (M7C3) precipitate (particle-like) decreased, and the amount of stable M7C3 carbides increased [21].

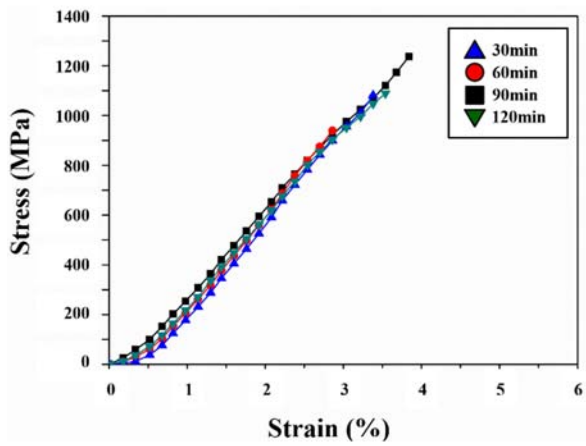

Figure 10. The strain-stress curve of the austempered specimens (1080 °C-30 min) with a salt-bath temperature of 300 °C and different salt-bath times.

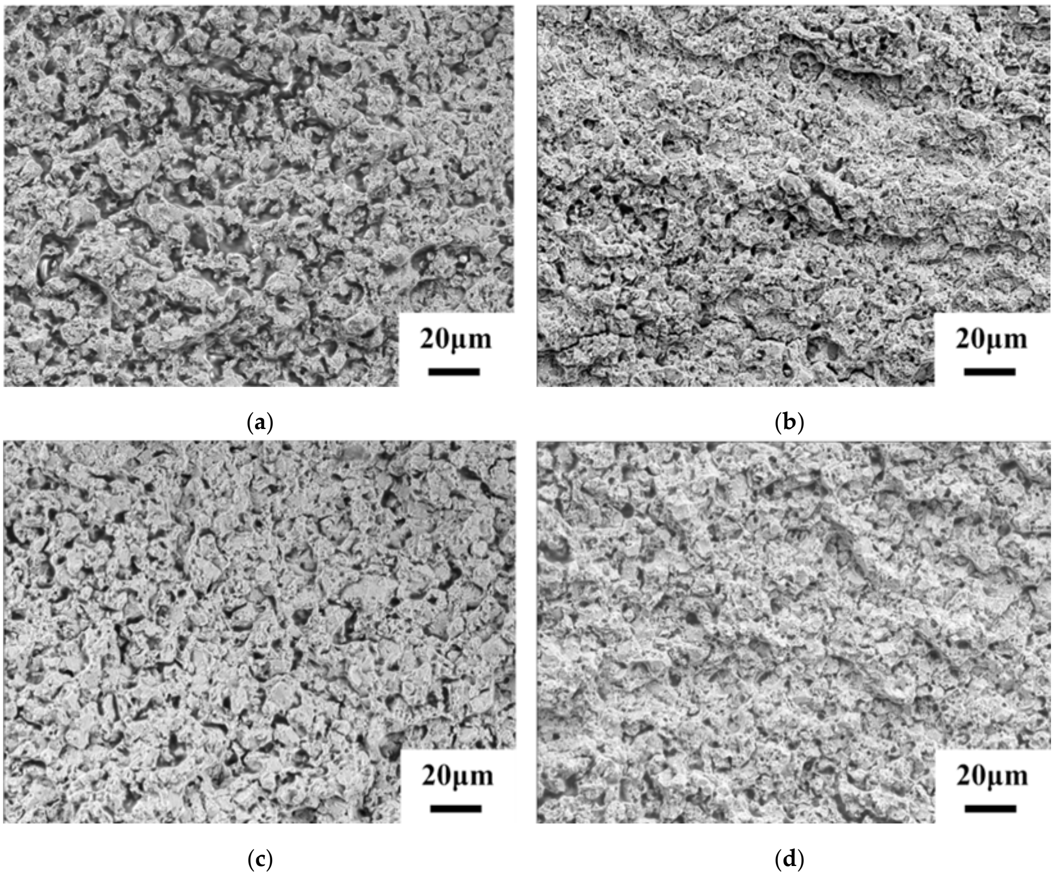

Figure 11. The fracture surfaces of the austempered specimens (1080 °C-30 min) with a salt-bath temperature of 300 °C and different salt-bath times: (**a**) 30 min, (**b**) 60 min, (**c**) 90 min, and (**d**) 120 min.

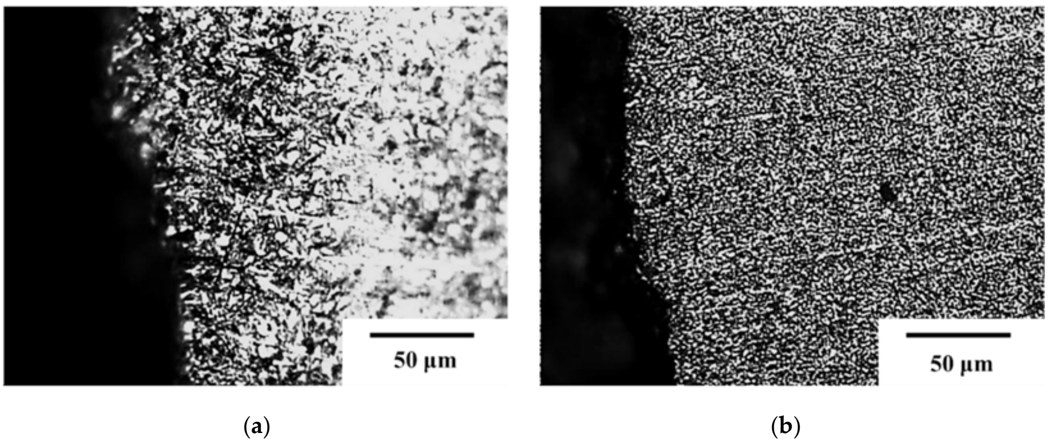

Figure 12. The subsurface of the austempered specimens (1080 °C-30 min) with a salt-bath temperature of 300 °C and different salt-bath times: (**a**) 30 min, and (**b**) 120 min.

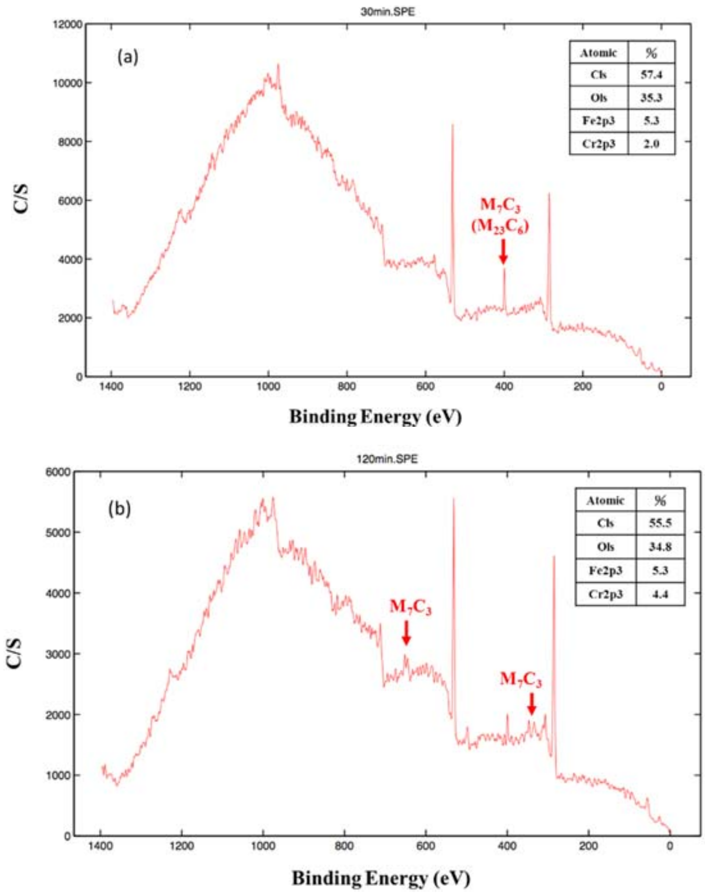

Figure 13. ESCA of carbides: (**a**) 30 min, and (**b**) 120min.

Figure 14 shows the mechanical properties of the corresponding microstructures at different salt-bath conditions. The bainite (high-retained austenite) with M7C3 coarsened as the salt-bath temperature increased. As the austempering time rose, the salt-bath condition of 300 °C-90 min, produced the specimen with the highest fracture strength. The results showed that an SUS440 thin plate with a suitable bainite matrix can have both lower brittleness and greater reliability with regard to the tensile mechanical properties.

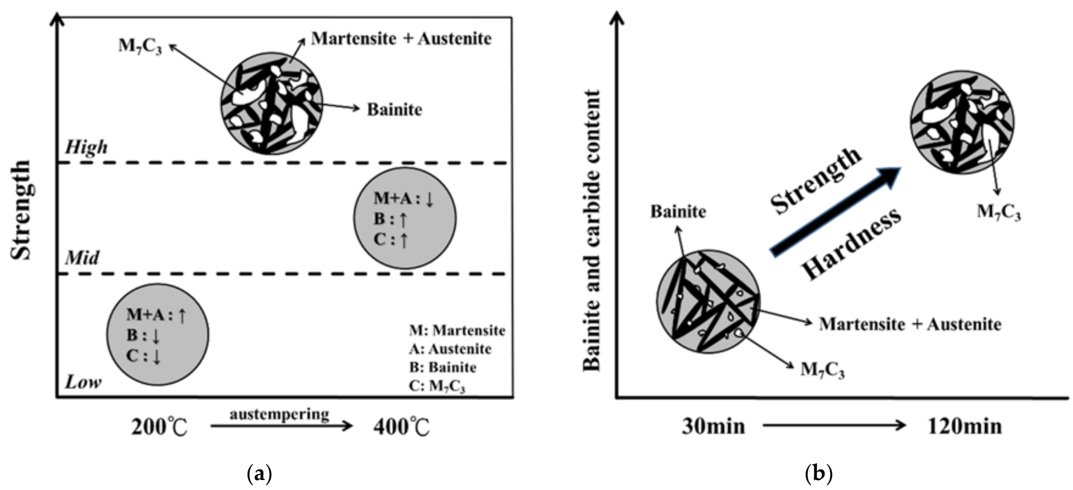

Figure 14. Diagram of tensile mechanical properties with different salt-bath conditions: (**a**) different salt-bath temperatures, and (**b**) different salt-bath times.

4. Conclusions

(1) The brittleness of an SUS440 thin plate produced with a short austempering time will increase due to the martensite phases in the matrix. A longer austempering time reduces the strength of the SUS440 thin plate due to changes in the content of retained austenite and M7C3 precipitate. The 300 °C-90 min specimen had the best mechanical properties.

(2) The martensite and retained austenite of the bainite matrix have a close relationship with the tensile brittleness of an SUS440 thin plate. The distribution of tempering M7C3 precipitate phases affected the failure mechanism.

Acknowledgments: The authors are grateful to The Instrument Center of National Cheng Kung University and 103-2221-E-006-066 for financial support for this research.

Author Contributions: C.-Y.C. and F.-Y.H. designed the research and wrote the manuscript with help from the other authors; C.-Y.C. performed the experiments and analyzed the data; F.-Y.H. C.-S.L. and L.-H.C. gave the support and comments.

Conflicts of Interest: The authors declare no conflict of interest.

References

1. Bee, J.V.; Powell, G.L.F.; Bednarz, B. A substructure within the austenitic matrix of high chromium white irons. *Scr. Metall. Mater.* **1994**, *31*, 1735–1736. [CrossRef]
2. Salleh, S.H.; Omar, M.Z.; Syarif, J. Carbide formation during precipitation hardening of SS440C steel. *Eur. J. Sci. Res.* **2009**, *34*, 83–91.
3. Lin, Y.L.; Lin, C.; Tsai, T. Microstructure and mechanical properties of 0.63C-12.7Cr martensitic stainless steel during various tempering treatments. *Mater. Manuf. Proc.* **2010**, *25*, 246–248. [CrossRef]
4. Salih, A.A.; Omar, M.Z.; Junaidi, S.; Sajuri, Z. Effect of different heat treatment on the SS440C martensitic stainless steel. *Aust. J. Basic Appl. Sci.* **2011**, *5*, 867–871.
5. Bhadeshia, H. Martensite and bainite in steels: Transformation mechanism & mechanical properties. *J. Phys. IV* **1997**, *7*, 367–376.
6. Lee, H.Y.; Yen, H.; Chang, H.; Yang, J. Substructures of martensite in Fe-1C-17Cr stainless steel. *Scr. Mater.* **2010**, *62*, 670–673. [CrossRef]
7. Salleh, S.H. Investigation of microstructures and properties of 440C martensitic stainless steel. *Int. J. Mech. Mater. Eng.* **2009**, *4*, 123–126.
8. Carpenter, S.D.; Carpenter, D. X-ray diffraction study of M7C3 carbide within a high chromium white iron. *Mater. Lett.* **2003**, *57*, 4456–4459. [CrossRef]
9. Carpenter, S.D.; Carpenter, D.; Pearce, J.T.H. XRD and electron microscope study of an as-cast 26.6% chromium white iron microstructure. *Mater. Chem. Phys.* **2004**, *85*, 32–40. [CrossRef]
10. Liu, C.; Zhao, Z.; Northwood, D.O.; Liu, Y. A new empirical formula for the calculation of M_S temperatures in pure iron and super-low carbon alloy steels. *J. Mater. Proc. Technol.* **2001**, *113*, 556–562. [CrossRef]
11. Chen, C.Y.; Hung, F.; Lui, T.; Chen, L. Microstructures and mechanical properties of austempering Cr-Mo (SCM 435) alloy steel. *Mater. Trans.* **2013**, *54*, 56–60. [CrossRef]
12. Tsuzaki, K.; Maki, T. Some aspects of bainite transformation in Fe-based alloys. *J. Phys. IV* **1995**, *5*, 61–70. [CrossRef]
13. Funatani, K. Low-temperature salt bath nitriding of steels. *Met. Sci. Heat Treat.* **2004**, *46*, 277–281. [CrossRef]
14. Lee, B.-J. On the stability of Cr carbides. *Calphad* **1992**, *16*, 121–149. [CrossRef]
15. Kwok, C.T.; Lo, K.; Cheng, F.; Man, H. Effect of processing conditions on the corrosion performance of laser surface-melted AISI 440C martensitic stainless steel. *Surf. Coat. Technol.* **2003**, *166*, 221–230. [CrossRef]
16. Carpenter, S.D.; Carpenter, D.; Pearce, J.T.H. XRD and electron microscope study of a heat treated 26.6% chromium white iron microstructure. *Mater. Chem. Phys.* **2007**, *101*, 49–55. [CrossRef]
17. Avishan, B.; Yazdani, S.; Nedjad, S.H. Toughness variations in nanostructured bainitic steels. *Mater. Sci. Eng. A* **2012**, *548*, 106–111. [CrossRef]
18. Luo, Y.; Peng, J.; Wang, H.; Wu, X. Effect of tempering on microstructure and mechanical properties of a non-quenched bainitic steel. *Mater. Sci. Eng. A* **2010**, *527*, 3433–3437. [CrossRef]

19. Yang, J.R.; Yu, T.H.; Wang, C.H. Martensitic transformations in AISI 440C stainless steel. *Mater. Sci. Eng. A* **2006**, *438*, 276–280. [CrossRef]
20. Sajjadi, S.A.; Zebarjad, S.M. Isothermal transformation of austenite to bainite in high carbon steels. *J. Mater. Proc. Technol.* **2007**, *189*, 107–113. [CrossRef]
21. Isfahany, A.N.; Saghafian, H.; Borhani, G. The effect of heat treatment on mechanical properties and corrosion behavior of AISI420 martensitic stainless steel. *J. Alloys Compd.* **2011**, *509*, 3931–3936. [CrossRef]